Article

Cell Reports

Intermediate Progenitor Cohorts Differentially Generate Cortical Layers and Require Tbr2 for Timely Acquisition of Neuronal Subtype Identity

Graphical Abstract

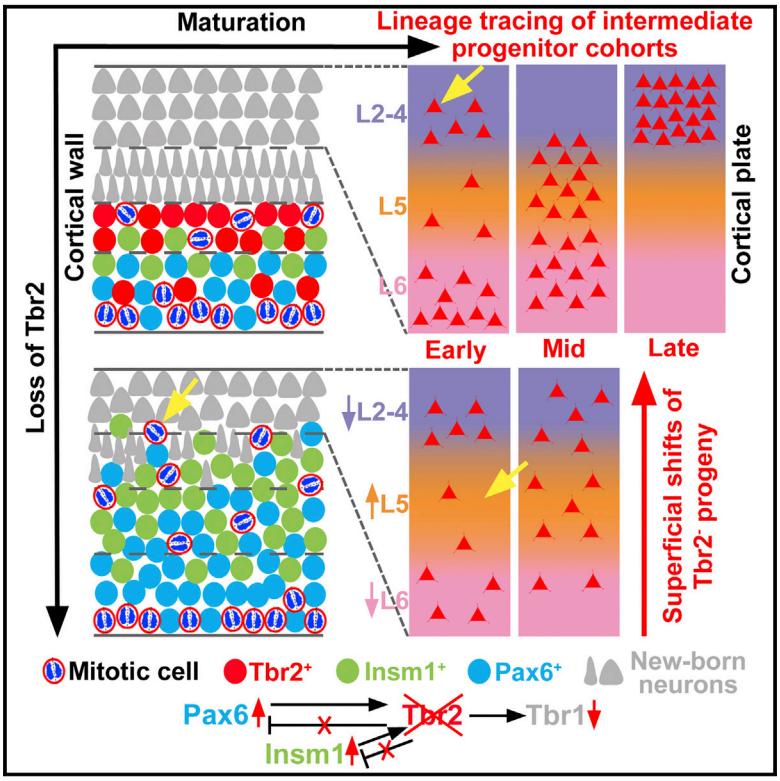

Highlights

- Intermediate progenitors (IPs) generate all types of cortical projection neurons
- A subset of early IPs produces upper-layer neurons
- Projection neuron laminar fates are dysregulated in the Tbr2-deficient cortex
- Tbr2 is mainly necessary for differentiation, not genesis, of IPs

Authors

Anca B. Mihalas, Gina E. Elsen, Francesco Bedogni, Ray A.M. Daza, Kevyn A. Ramos-Laguna, Sebastian J. Arnold, Robert F. Hevner

Correspondence

rhevner@uw.edu

In Brief

The role of intermediate progenitors (IPs) in corticogenesis has been unclear. Mihalas et al. show that early IP cohorts produce lower- and upper-layer neurons and that Tbr2 is required to regulate differentiation, not genesis, of IPs.

Mihalas et al., 2016, Cell Reports *16*, 92–105
June 28, 2016
http://dx.doi.org/10.1016/j.celrep.2016.05.072

OPEN ACCESS
CellPress

Cell Reports
Article

Intermediate Progenitor Cohorts Differentially Generate Cortical Layers and Require Tbr2 for Timely Acquisition of Neuronal Subtype Identity

Anca B. Mihalas,[1] Gina E. Elsen,[1] Francesco Bedogni,[1,6] Ray A.M. Daza,[1] Kevyn A. Ramos-Laguna,[1] Sebastian J. Arnold,[2,3,4] and Robert F. Hevner[1,5,*]
[1]Center for Integrative Brain Research, Seattle Children's Research Institute, Seattle, WA 98101, USA
[2]Renal Department, University Medical Centre and Faculty of Medicine, University of Freiburg, 79106 Freiburg, Germany
[3]Institute of Experimental and Clinical Pharmacology and Toxicology and Faculty of Medicine, University of Freiburg, 79102 Freiburg, Germany
[4]BIOSS Centre of Biological Signaling Studies, University of Freiburg, 79104 Freiburg, Germany
[5]Department of Neurological Surgery, University of Washington School of Medicine, Seattle, WA 98104, USA
[6]Present address: San Raffaele Rett Research Unit, Division of Neuroscience, San Raffaele Scientific Institute, 20132 Milan, Italy
*Correspondence: rhevner@uw.edu
http://dx.doi.org/10.1016/j.celrep.2016.05.072

SUMMARY

Intermediate progenitors (IPs) amplify the production of pyramidal neurons, but their role in selective genesis of cortical layers or neuronal subtypes remains unclear. Using genetic lineage tracing in mice, we find that IPs destined to produce upper cortical layers first appear early in corticogenesis, by embryonic day 11.5. During later corticogenesis, IP laminar fates are progressively limited to upper layers. We examined the role of Tbr2, an IP-specific transcription factor, in laminar fate regulation using *Tbr2* conditional mutant mice. Upon *Tbr2* inactivation, fewer neurons were produced by immediate differentiation and laminar fates were shifted upward. Genesis of subventricular mitoses was, however, not reduced in the context of a *Tbr2*-null cortex. Instead, neuronal and laminar differentiation were disrupted and delayed. Our findings indicate that upper-layer genesis depends on IPs from many stages of corticogenesis and that Tbr2 regulates the tempo of laminar fate implementation for all cortical layers.

INTRODUCTION

Excitatory, pyramidal neurons of the cerebral cortex are generated during embryonic neurogenesis from radial glial progenitors (RGPs) both directly and indirectly via transient-amplifying, committed neurogenic intermediate progenitors (IPs) (reviewed by Florio and Huttner, 2014; Sun and Hevner, 2014). Importantly, the generation of neurons of different cortical layers follows a general "inside-out" pattern as lower layer (LL) neurons are born first and upper layers (ULs) last (Hevner et al., 2003).

IPs are distinguished from RGPs by short radial or multipolar morphology, mitotic division tending to occur away from the ventricular surface, and a unique molecular profile, including specific expression of the Tbr2 transcription factor (also known as Eomes; NCBI gene *Eomes*; Englund et al., 2005; Gal et al., 2006; Kawaguchi et al., 2008; Stancik et al., 2010). Given their distinct properties, IPs have been proposed to generate specific cortical neuron subtypes. However, the precise contribution of IPs to cortical neurogenesis and laminar fate specification remains poorly defined. Previously, IPs were suggested to produce mainly UL neurons (Tarabykin et al., 2001; Zimmer et al., 2004; Britanova et al., 2005), but further studies indicated that IPs produce all layers (Kowalczyk et al., 2009; Vasistha et al., 2015). More recently, the morphological and electrophysiological properties of UL neurons were reported to depend on their origins from Tbr2-negative RGPs or from Tbr2-positive IPs (Tyler et al., 2015). Thus, one goal of the present study was to use a panel of molecular markers to more extensively define neuron subtypes produced from IPs.

The second goal of the present study was to determine whether IPs generate cortical layers in a predetermined sequential order, depending on the time point of their generation, or whether individual IP cohorts may contribute to multiple layers. Previously, early IPs were observed to rapidly differentiate and produce LL neurons (Kowalczyk et al., 2009), but the possibility that some early IPs differentiate slowly and contribute to ULs has not been thoroughly investigated. The latter scenario could arise if some early IPs are restricted to UL fates, as reported for some early RGPs (Franco et al., 2012), or if some early IPs remain in the mitotic cycle for a protracted period before differentiating, as suggested for late IPs (Wu et al., 2005). We studied these possibilities by inducible genetic fate mapping using *Tbr2*^{CreER}, which, together with the reporter gene *Ai14*, specifically labels IPs and their progeny (Pimeisl et al., 2013).

To investigate regulation of laminar fate in IPs, we studied mice lacking Tbr2. Previously, it was reported that Tbr2-deficient cortex had decreased thickness of ULs, suggesting that Tbr2 promotes UL neuron fates (Arnold et al., 2008; Sessa et al., 2008). Here, we characterized the effects of Tbr2 deficiency on laminar fates of early, middle, and late IP cohorts. We studied IP genesis, migration, differentiation, and fates using molecular markers,

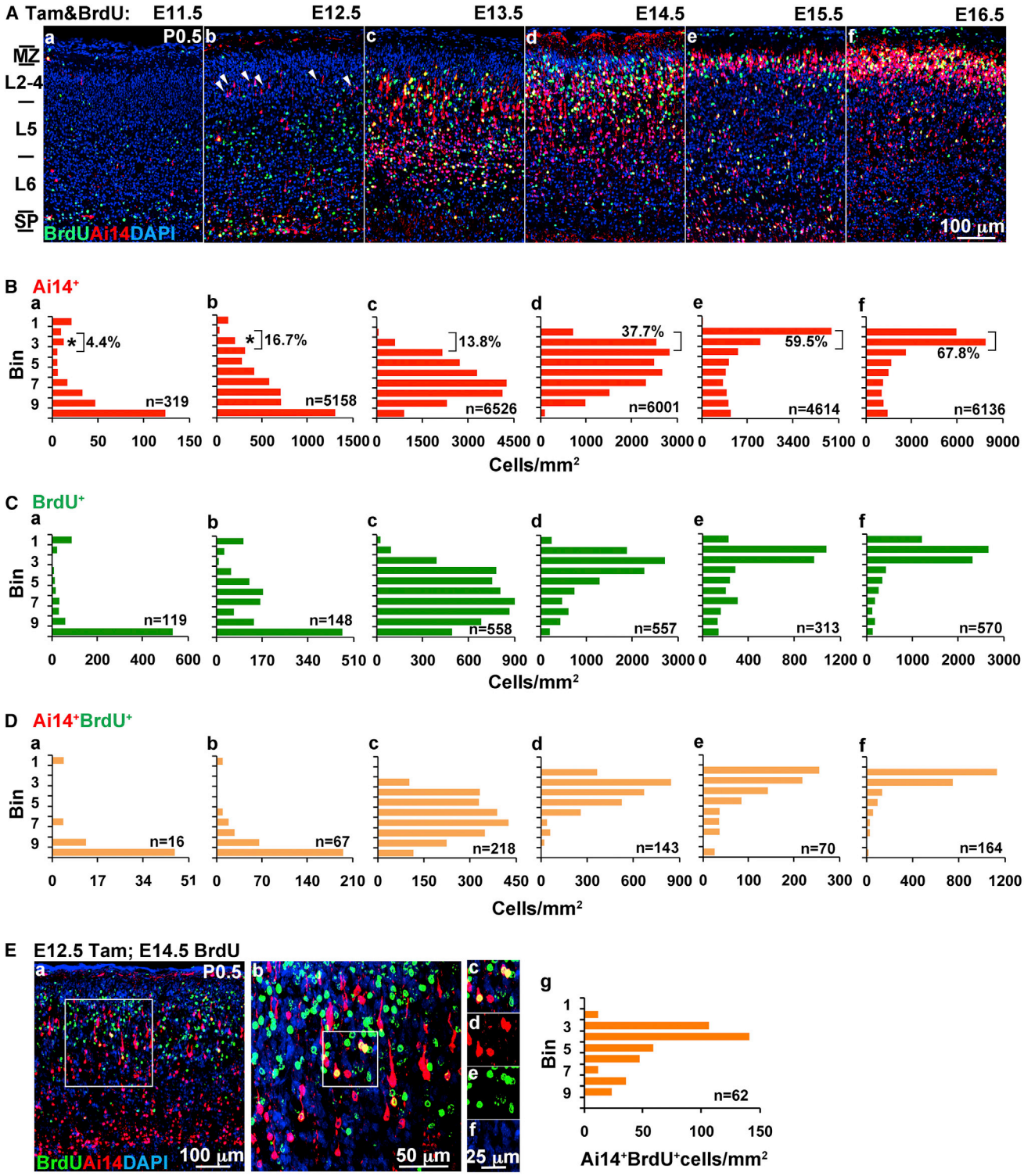

Figure 1. Laminar Fates and Birthdays of IP-Derived Progeny

(Aa–Af) Representative images of Ai14$^+$ and BrdU$^+$ cells from P0.5 pups injected with Tam and BrdU on different days from E11.5–E16.5. DAPI counterstain (blue) is shown. Cells were counted in bins from marginal zone (MZ) to subplate (SP). Typically, bin 1 represents the MZ, bins 2–3 are layers 2–4, bins 4–6 are layer 5, bins 7–9 are layer 6, and bin 10 is SP. The scale bar represents 100 μm.

(Ba–Bf) Bin analysis of Ai14$^+$ cells.

(Ca–Cf) Bin analysis of BrdU$^+$ cells.

(legend continued on next page)

lineage tracing, and cell birth dating. Unexpectedly, we found that Tbr2 is not required for genesis of subventricular IPs from RGPs as reported previously (Sessa et al., 2008) but is required mainly for differentiation of IPs to projection neurons, including acquisition of LL and UL identities.

Our results show that sequential cohorts of IPs generate progressively limited sets of cortical layers, such that UL neurogenesis depends not only on late but also on early generated IPs. Furthermore, the process of laminar neurogenesis from IPs is regulated by Tbr2, which controls the tempo of LL and UL differentiation. Thus, in addition to previously described roles to control cortical regional patterning (Elsen et al., 2013), IPs and Tbr2 play important roles in laminar differentiation of the cerebral cortex.

RESULTS

Some Early IPs Produce UL Neurons

To label IP cohorts and their progeny, we used *Tbr2*^{CreER};*Ai14* mice (Pimeisl et al., 2013), in which tamoxifen (Tam) administration induces permanent expression of tdTomato, a red fluorescent protein (RFP), in *Tbr2*-expressing cells and their progeny. Tam was administered on embryonic days 11.5 (E11.5)–E16.5, and brains were collected on postnatal day (P) 0.5 (Figure S1). To identify neurons born on the day of Tam administration, bromodeoxyuridine (BrdU) was given concurrently (Figure 1).

Lineage tracing revealed that IP cohorts contributed differentially to cortical layers (Figures 1A and 1B). Early IP cohorts (E11.5–E12.5) generated not only LL neurons as expected from BrdU birth dating (Figures 1B–1D) but also substantial numbers of UL neurons. Indeed, neurons derived from E11.5–E12.5 IPs were distributed bimodally in LLs and ULs, and as many as 17% of the RFP$^+$ neurons generated from E12.5 IPs settled in ULs (Figures 1Ba and 1Bb). Whereas LL neurons derived from early IPs were early born, the UL neurons derived from early IPs were not early born, as they did not incorporate BrdU given concurrently with Tam (Figures 1Da and 1Db).

IPs from mid-neurogenesis (E13.5–E14.5) contributed widely to LLs and ULs, whereas late IPs (E15.5–E16.5) produced ULs selectively (Figures 1A–1D).

Early IPs Produce Diverse Molecular Subtypes of Cortical Projection Neurons

Because UL neurons are generally born later in neurogenesis (Hevner et al., 2003), we considered the possibility that some early IPs (E12.5) do not undergo final mitosis until much later in neurogenesis. To test this hypothesis, we administered Tam on E12.5 and BrdU on E14.5, followed by survival to P0.5. With this schema, many double-labeled (RFP$^+$/BrdU$^+$) neurons were detected in ULs (but not LLs), confirming that some early IPs persisted for at least 2 embryonic days before final mitosis (Figure 1E). However, we do not know whether the early IPs divided only once or repeatedly during this period.

Cortical projection neurons are defined by not only laminar position but also molecular expression (Hevner et al., 2003; Molyneaux et al., 2007). To further identify the neuron subtypes produced from E12.5 IPs, we evaluated their expression of Reelin, a Cajal-Retzius (C-R) cell marker; Tbr1, expressed at high levels in layer 6 (L6); Ctip2 (L5); Satb2 (callosal projection neurons); Cux1 (L2–4); and Dlx (interneuron precursors; Figure S2). Remarkably, E12.5 IPs produced all five subtypes of projection neurons (Figure S3). As expected, no IP-derived neurons expressed Dlx (data not shown; see also Figures 2L and 2L′).

Progressive Limitation of IP Laminar and Molecular Fates

To molecularly characterize the subtypes of projection neurons produced by sequential IP cohorts, we extended our analysis to include E11.5–E16.5 IP cohorts (Figure 2). C-R cells (Reelin$^+$) were produced from early IPs (E11.5–E12.5) only (Figures 2A, 2A′, and 2F). LL neurons (Tbr1$^+$ or Ctip2$^+$) were produced from early to middle (E11.5–E14.5) IPs only. In contrast, UL neurons (Cux1$^+$) and callosal projection neurons (Satb2$^+$) were produced from all IP cohorts (Figure 2). Some RFP$^+$ progeny of late IPs (E15.5–E16.5) were located in LLs on P0.5 (Figures 1Ae, 1Af, 2E, and 2L), but these appeared to be migrating neurons destined for ULs, as they had elongated morphologies and did not express LL markers (Figure S4). Thus, at the population level, early IPs exhibit diverse laminar and molecular fates, whereas later IP cohorts have progressively limited fates.

The interpretation of fates from E11.5–E12.5 IPs was complicated by the fact that, at these ages, Tbr2 is expressed by not only IPs but also postmitotic C-R and subplate (SP) neurons (Englund et al., 2005). Thus, C-R and SP neurons may be labeled by Tam treatment on E11.5 or E12.5, even if these neurons were not derived from IPs. To verify the origins of C-R and SP neurons from IPs, we injected Tam and BrdU on E11.5 and studied cortex on E15.5. Triple-label immunofluorescence (IF) demonstrated that many Reelin$^+$ C-R cells, and calretinin$^+$ SP neurons, were labeled with RFP and BrdU, confirming their origins from proliferating Tbr2$^+$ IPs (Figures 2M and 2N). Thus, IPs produce preplate (C-R and SP) as well as LL and UL projection neuron subtypes.

Tbr2-Deficient Early IPs Produce Fewer Rapidly Differentiating Neurons

To test whether Tbr2 regulates laminar fate in IPs cell autonomously, we utilized *Tbr2*^{CreER} to inactivate floxed *Tbr2* (*Tbr2*^{FL}; Intlekofer et al., 2008) in IP cohorts. Administration of Tam to *Tbr2*$^{CreER/FL}$;*Ai14* mice resulted in RFP labeling of Tbr2-deficient IPs and their progeny. (However, IPs presumably expressed functional Tbr2 transiently before *Tbr2*^{FL} was recombined.) We labeled cohorts of Tbr2-deficient IPs on E12.5 or E14.5 and

(Da–Df) Bin analysis of Ai14$^+$/BrdU$^+$ double-positive neurons, born from IPs that last divided on the BrdU/Tam injection day. The n represents the total number of cells included in the analysis. n = 2–4 embryos for each time point of Tam induction.
(E) Diverse latency to last division. Whereas many E12.5 IPs (RFP labeled by Tam injection on E12.5) exited the cell cycle on E12.5 (Db), others did not divide finally until E14.5, as shown by E14.5 BrdU labeling with survival to P0.5. (Ea–Ef) Double-labeled Ai14$^+$/BrdU$^+$ neurons seen by confocal microscopy are shown. (Eg) Bin analysis of Ai14$^+$/BrdU$^+$ cells showed these neurons occupied mainly ULs. (Some Ai14$^+$/BrdU$^+$ cells in lower layers were still migrating.) n = 2 embryos.
Also see Figure S1.

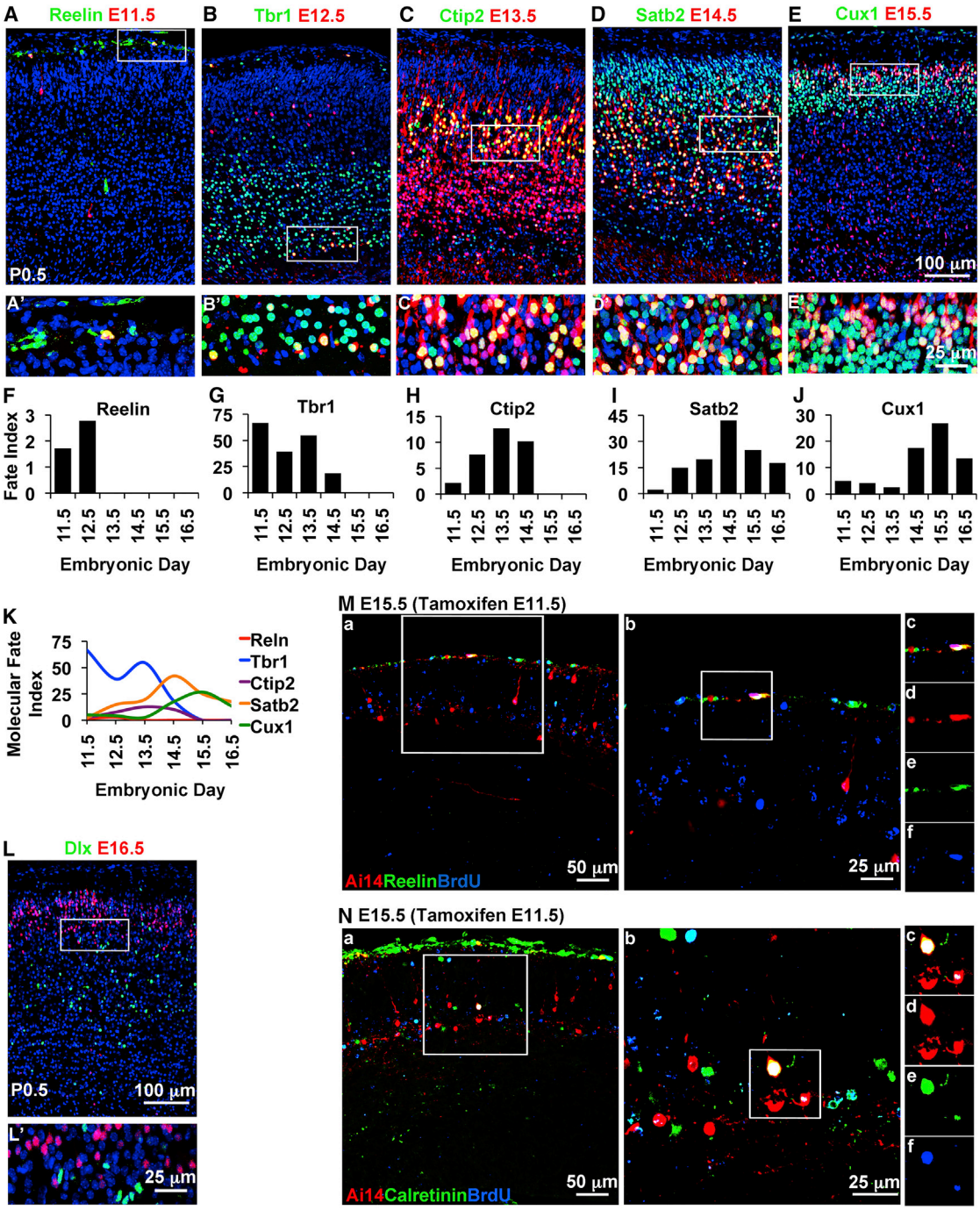

Figure 2. IP Cohorts Produce All Types of Projection Neurons in Overlapping Sequence

(A–E) Different IP cohorts showed distinct profiles of neurogenesis and different predominant fates. In these images, neurons from different IP cohorts are shown with selected colocalized molecular markers in P0.5 cortex: (A) E11.5 Tam, Reelin; (B) E12.5 Tam, Tbr1; (C) E13.5 Tam, Ctip2; (D) E14.5 Tam, Satb2; and (E) E15.5 Tam, Cux1. The scale bar represents 100 μm. (A′–E′) Higher magnification of boxed areas in (A)–(E). The scale bar represents 25 μm.

(F–J) Different neuron types were produced with different frequency from different IP cohorts. For each molecular type of neuron, the fate index (% of Ai14$^+$ cells that express a marker) changed with each sequential IP cohort, revealing a profile of neurogenesis.

(K) Summary of molecular fate index profiles from different IP cohorts.

(L) IPs did not produce Dlx$^+$ interneurons on E16.5 (shown) or any other ages.

(M and N) Some C-R and SP neurons were produced from IPs. Tam and BrdU were administered on E11.5, with survival to E15.5. IP-derived C-R neurons (Reelin$^+$/BrdU$^+$/Ai14$^+$) were located in the MZ and SP neurons (Calretinin$^+$/BrdU$^+$/Ai14$^+$) in the morphological SP. The scale bars represent (a) 50 μm and (b–f) 25 μm.

Also see Figures S2–S4.

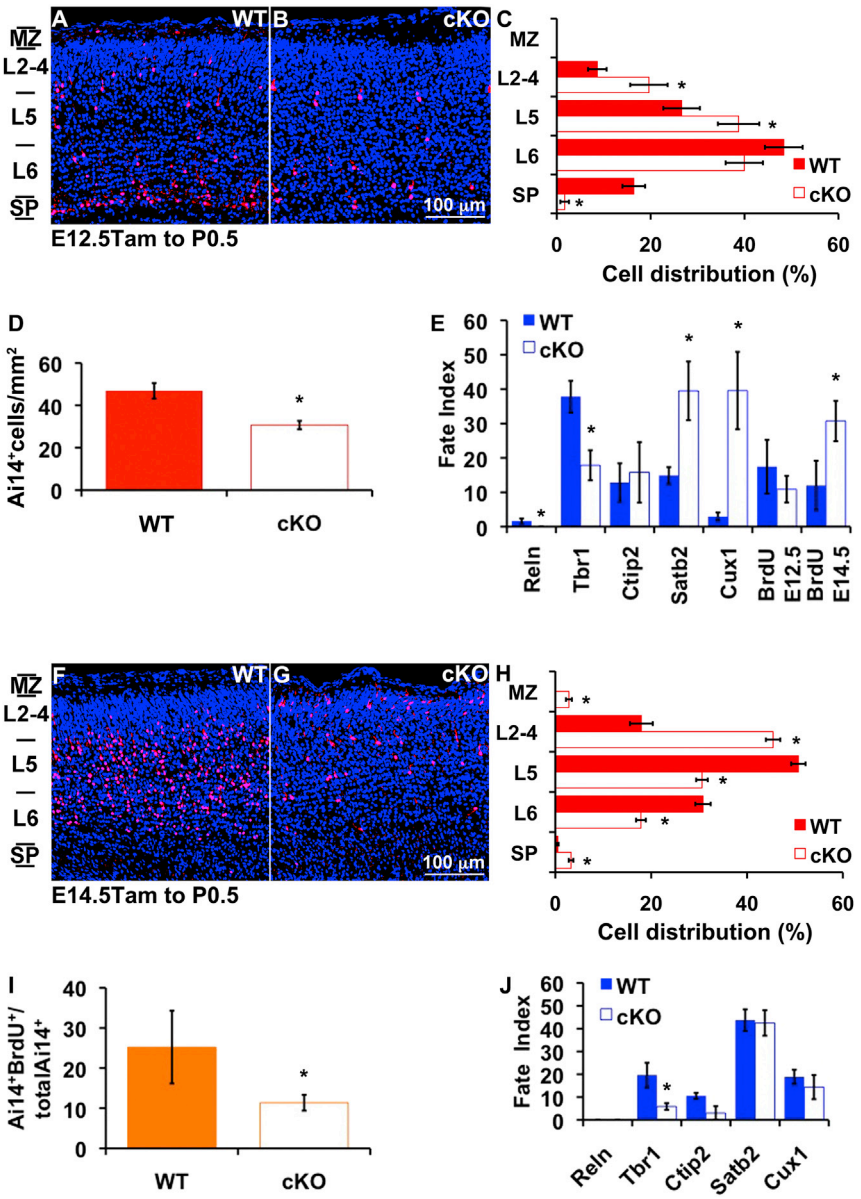

Figure 3. Tbr2-Deficient IP Cohorts Shift to More-Superficial Laminar Fates

Tbr2^{CreER} was used for both lineage tracing and *Tbr2* inactivation in IP cohorts.

(A–E) Neurogenesis of RFP$^+$ neurons from E12.5 IPs was reduced and shifted after *Tbr2* inactivation. (A) Control experiment showing E12.5 IP-derived, Ai14$^+$ neurons in P0.5 cortex. (B) Tbr2-deficient IPs produced fewer neurons overall, with marked loss of LL fates and relative sparing of UL fates. (C) Cortical layer analysis (assignment of cortical layers was rendered from ten equidistant bins spanning from pial surface to SP, as described in Figure 1 legend) showed that Tbr2-deficient E12.5 IPs produced Ai14$^+$ neurons that were shifted superficially in the CP (*$p \leq 0.043$). (D) Tbr2-deficient E12.5 IPs produced approximately 35% fewer neurons overall ($p = 3.9 \times 10^{-4}$). (E) The molecular fates and cell birthdays of neurons derived from Tbr2-deficient E12.5 IPs were shifted. Tbr2-deficient IPs produced fewer (none) Reelin$^+$ ($p = 0.006$) C-R neurons and fewer Tbr1$^+$ L6 neurons ($p = 0.015$) but relatively more Cux1$^+$ ($p = 0.01$) and Satb2$^+$ ($p = 0.02$) neurons. Neurons from Tbr2-deficient IPs were also more likely to be born later, on E14.5 ($p = 0.049$). n = 4 WT and 4 cKO embryos.

(F–J) Neurogenesis from E14.5 IPs was reduced and superficially shifted after *Tbr2* inactivation (survival to P0.5). Compared to controls (F), Tbr2-deficient E14.5 IPs (G) produced fewer LL neurons and more neurons in the superficial CP. (H) Cortical layer analysis confirmed the gain of UL fates (L2–4; $p = 6.7 \times 10^{-13}$) and loss of LL fates (L5 and 6; $p \leq 1.4 \times 10^{-8}$). (I) E14.5 Tam and BrdU administration is shown. Less than half as many Tbr2-deficient E14.5 IPs had their last division at E14.5 ($p = 0.035$). (J) Molecular fate analysis showed that Tbr2-deficient E14.5 IPs produced fewer Tbr1$^+$ L6 neurons ($p = 0.014$). n = 2 WT and 3 cKO embryos. The scale bar represents 100 μm (all images). Error bars indicate SEM.

evaluated RFP$^+$ progeny on P0.5. Control mice were treated identically but lacked the *Tbr2*^{FL} allele (i.e., *Tbr2*$^{CreER/+}$;*Ai14*).

Tbr2-deficient E12.5 IPs produced significantly fewer total neurons than did control E12.5 IPs (control = 49 ± 4 cells/mm^2; conditional knockout [cKO] = 31 ± 2 cells/mm^2; $p = 0.0004$; Figures 3A–3D). Among Tbr2-deficient IPs, fewer became SP neurons (wild-type [WT] = 16.4% ± 2%; cKO = 1.6% ± 1%; $p = 7.1 \times 10^{-7}$), whereas more became L5 neurons (WT = 27% ± 3%; cKO = 39% ± 4%; $p = 0.043$) and L2–4 neurons (WT = 9% ± 2%; cKO = 20% ± 4%; $p = 0.0145$; Figures 3A–3C). The upward laminar shift of neurons from Tbr2-deficient IPs was matched by genesis of fewer Tbr1$^+$ SP neurons (WT = 38% ± 5%; cKO = 18% ± 4%; $p = 0.0154$) but increased numbers of Satb2$^+$ callosal projection neurons (WT = 15% ± 2%; cKO = 40% ± 8%; $p = 0.0209$) and Cux1$^+$ UL neurons (WT = 3% ± 1%; cKO = 40% ± 11%; $p = 0.0104$). Also, Tbr2-deficient E12.5 IPs were more likely to delay final division until E14.5 (WT = 12% ± 7%; cKO = 30.7% ± 6%; $p = 0.0493$; Figure 3E). Thus, E12.5 IPs require Tbr2 mainly for genesis of early-born LL neuron subtypes, but not for later-born callosal and UL neuron subtypes.

The effects of Tbr2 deficiency on E14.5 IPs were broadly similar as on E12.5 IPs. Laminar fates were shifted upward (Figures 3F–3H), with more IP-derived neurons distributed in ULs 2–4 (WT = 18% ± 2%; cKO = 45.4% ± 2%; $p = 6.7 \times 10^{-13}$) and fewer in L5 (WT = 50.7% ± 2%; cKO = 30.6% ± 1%; $p = 2.7 \times 10^{-12}$) and L6 (WT = 30.8% ± 2%; cKO = 17.9% ± 1%; $p = 1.4 \times 10^{-8}$). Also, Tbr2-deficient E14.5 IPs produced fewer Tbr1$^+$ (SP/L6) neurons (WT = 19.7% ± 5%; cKO = 5.9% ± 1%; $p = 0.0144$) and were less likely to differentiate rapidly on E14.5 (WT = 25.2% ± 9%; cKO = 11.4% ± 2%; $p = 0.0357$; Figures 3I and 3J).

Together, these results suggest that Tbr2 is necessary for differentiation of IPs to produce rapidly generated neuron types. The shift to genesis of later-generated neuron types from Tbr2-deficient IPs may result from delayed differentiation related to molecular dysregulation (see below).

Shifts of Neurogenesis and Laminar Fates in Tbr2-Deficient Cortex

We next investigated the effects of complete *Tbr2* deficiency on cortical neurogenesis. To produce mice lacking Tbr2 in the nervous system, we recombined $Tbr2^{FL}$ using $Nes11^{Cre}$ (Tronche et al., 1999). For simplicity, we designated the $Nes11^{Cre}$;$Tbr2^{FL/FL}$ mice as *Tbr2* cKO mutants.

To profile the timing of neurogenesis in control and *Tbr2* cKO cortex, we labeled early- (E12.5), middle- (E14.5), or late-born (E16.5) neurons with BrdU and studied the distribution of $BrdU^+$ cells after survival to P2. As expected from lineage tracing of Tbr2-deficient IPs (Figure 3), neurogenesis was moderately decreased in *Tbr2* cKO cortex on E14.5 (79% of control; $p = 0.016$) and E16.5 (71% of control; $p = 0.06$), whereas the laminar fates of these cells were unchanged or shifted slightly upward (Figures 4B and 4C). In contrast, the genesis of E12.5-born neurons was significantly increased by 2.3-fold ($p = 0.0001$) in *Tbr2* cKO cortex (Figure 4A).

The increased genesis of E12.5-born neurons in *Tbr2* cKO cortex suggested that SP and L6 thickness might be increased postnatally, as SP and L6 are the major neuron types born on E12.5 in normal mice (Figure 1C). Instead, we found significant expansion of L5 ($Ctip2^+$) neurons (1.7-fold; $p = 3.2 \times 10^{-8}$), at the expense of SP/L6 ($Tbr1^+$; 76%; $p = 0.0008$) and L2–4 ($Cux1^+$; 50%; $p = 0.0124$) neurons (Figures 4D and 4E). Thus, approximately twice as many E12.5-born cells differentiated as $Ctip2^+$ L5 neurons ($p = 0.0139$) in *Tbr2* cKO mutants as in controls (Figure S5B). These results indicated that the relation between cell birthday and laminar fate was perturbed in *Tbr2* cKO cortex. Interestingly, one previous study also reported slight expansion of L5 in *Tbr2* cKO cortex, although not statistically significant (Arnold et al., 2008).

Tbr2 cKO Mice Have Small Brains but No Deficits of Simple Motor Skills

Tbr2 cKO mice survived to adulthood but had 20%–30% reduced body and brain mass (Figures S5F–S5J). (The causes of reduced body mass in *Tbr2* cKO mice remain uncertain but could include reduced feeding, hyperactivity, or hormonal changes.)

To evaluate motor development, we used rotarod and balance beam tests. Paradoxically, *Tbr2* cKO mice had enhanced performance on both tests, although the enhancement declined in older mutants (Figures S5C and S5E). Importantly, body size did not correlate with motor performance ($R^2 < 0.02$; Figure S5D), so the enhancement in *Tbr2* cKO mutants cannot be attributed to lower body mass.

Other brain abnormalities in *Tbr2* cKO mice included severe olfactory bulb hypoplasia and reduced cortical surface area (Figures S5H and S5J; see also Arnold et al., 2008). In contrast, cortical thickness was not significantly reduced (Figure 4). Also, the anterior commissure was absent, although the corpus callosum and hippocampal commissure showed no obvious defects (Figures S6G and S6H; see also Hodge et al., 2013).

Gene Dysregulation in *Tbr2* cKO IPs and Neuronal Progeny

To investigate molecular defects in *Tbr2* cKO mutants, we analyzed microarray data comparing E14.5 WT and *Tbr2* cKO neocortex from our previous study, which focused on rostrocaudal identity (Elsen et al., 2013). Here, we focused on critical genes in neurogenesis and laminar fate acquisition. Genes up- or downregulated in *Tbr2* cKO neocortex were identified by positive or negative $\log_2$FC ($\log_2$ of the fold change) values, indicating significant differences ($p < 0.05$) between *Tbr2* cKO and control cortex.

Interestingly, transcription factor (TF) genes "upstream" of *Tbr2* were upregulated in *Tbr2* cKO cortex, including *Pax6* ($\log_2$FC = +0.36; $p = 0.001$) and *Insm1* ($\log_2$FC = +0.46; $p = 0.001$). In contrast, "downstream" markers of laminar differentiation were mixed, with downregulation of *Tbr1* ($\log_2$FC = −0.78; $p = 0.00004$), *Bcl11b/Ctip2* ($\log_2$FC = −0.38; $p = 0.009$), and *Satb2* ($\log_2$FC = −1.47; $p = 0.00008$) but upregulation of *Zfpm2/FOG2* ($\log_2$FC = +0.63; $p = 0.0005$) and *Adcyap1/PACAP* ($\log_2$FC = +1.49; $p < 10^{-7}$). Interestingly, both *Tbr1* and *FOG2* are L6 markers (Bedogni et al., 2010), but they were regulated in opposite directions on E14.5, as were L5 markers *Ctip2* and *PACAP*. These data suggested that differentiation of postmitotic neurons was severely dysregulated in *Tbr2* cKO cortex.

All Stages of Cortical Differentiation Are Abnormal in *Tbr2* cKO Cortex

To further investigate the differentiation defects inferred from microarray analysis, we studied the expression of neuronal differentiation markers by IF. This approach allowed us to define not only quantitative changes in gene expression but also qualitative changes in zonal differentiation patterns (Bystron et al., 2008).

Patterns of neuron differentiation were profoundly disturbed in E14.5 *Tbr2* cKO cortex (Figure 5). The cortical plate (CP) and intermediate zone (IZ) appeared thin, and fewer cells expressed markers of postmitotic LL ($Tbr1^+$; 67%; $p = 0.0126$) and callosal ($Satb2^+$; 9%; $p = 5.9 \times 10^{-6}$) differentiation (Figures 5A and 5B). In contrast, FOG2 (L6; 1.5-fold increase; $p = 0.0038$) and Ctip2 (L5; 83% decrease; $p = 0.0441$), which are restricted to the CP on E14.5 in WT embryos, showed ectopic expression in the IZ of *Tbr2* cKO mutants (Figures 5C and 5D). $PACAP^+$ cells, representing a subset of L5 neurons (Lodato et al., 2014), were more abundant and more immunoreactive in the *Tbr2* cKO CP (Figure 5E). C-R neurons ($Reelin^+$) appeared slightly increased in *Tbr2* cKO mice (data not shown), similarly as in *Pax6* mutants (Stoykova et al., 2003). Together, these results demonstrated that projection neuron differentiation was severely disorganized and dysregulated in E14.5 *Tbr2* cKO mutants.

To further characterize the trajectory of cortical differentiation in *Tbr2* cKO cortex, we studied E12.5 and E16.5 time points (Figure S6). In E12.5 mutants, the preplate appeared thicker than normal, due to an abundance of $NeuroD^+/Tbr1^-$ immature neurons, along with approximately normal numbers of $Tbr1^+$ neurons (Figures S6A and S6B). Interestingly, the boundary between VZ ($Sox2^+$) and preplate ($Tbr1^+$) appeared irregular due to the

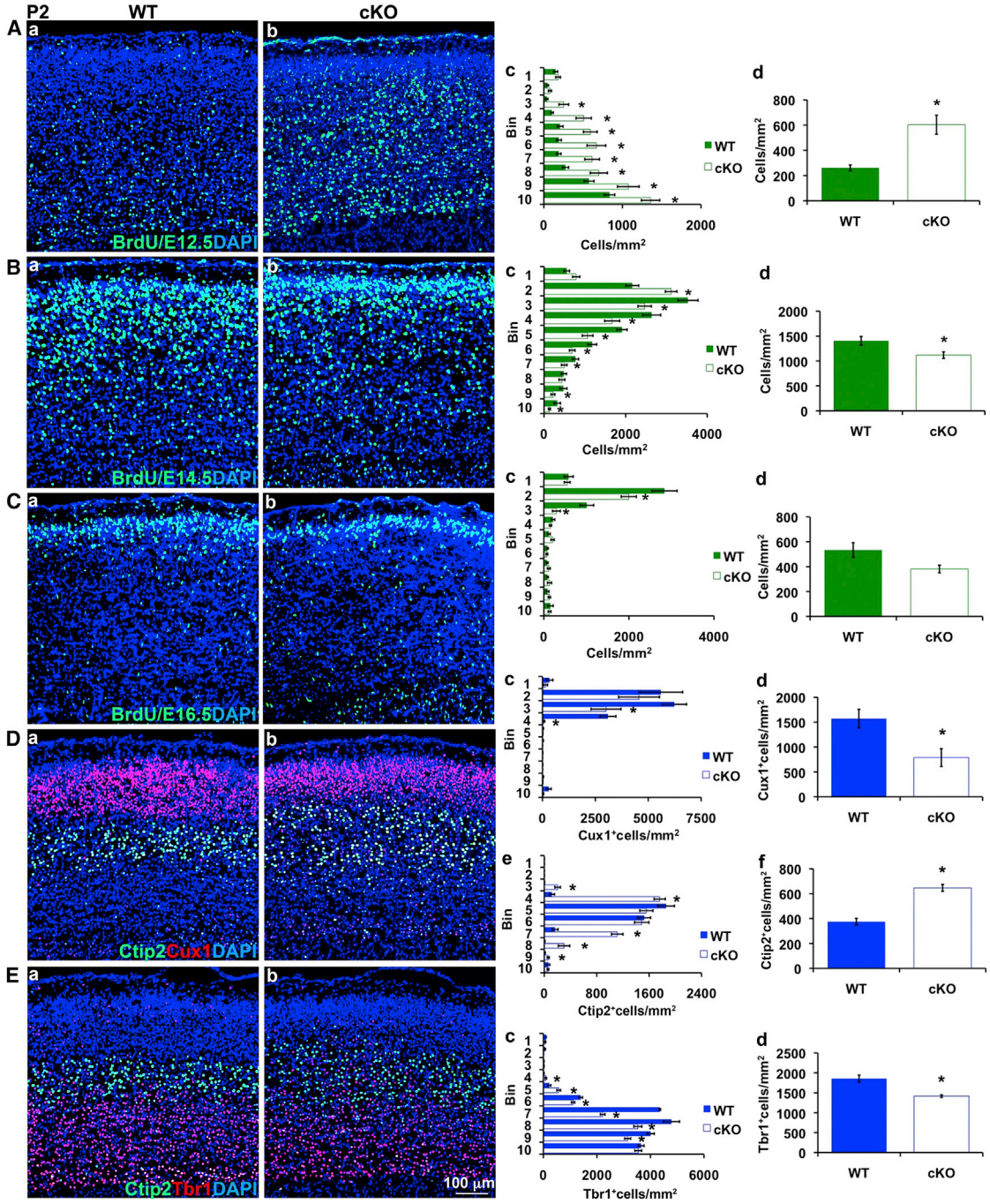

Figure 4. *Tbr2* cKO Cortex Shows Precocious Neurogenesis and Increased Layer 5 Thickness

(A–C) BrdU birth dating (with survival to P2) showed that, compared to controls (Aa, Ba, and Ca), *Tbr2* cKO mice (Ab, Bb, and Cb) had increased early neurogenesis (A; E12.5; $p = 1.4 \times 10^{-4}$), followed by decreased middle (B; E14.5; $p = 0.016$) and late (C; E16.5; $p = 0.061$) neurogenesis. Bin analysis (Ac, Bc, and Cc) showed shifts of laminar fate (*$p < 0.045$), and cell counts confirmed changes in overall neurogenesis (Ad, Bd, and Cd). Interestingly, early neurogenesis in *Tbr2* cKO mice was shifted to increased genesis of middle bins, corresponding to layer 5 of P2 cortex (Ac).

(D and E) *Tbr2* cKO mice have increased layer 5 thickness, at the expense of layers 6 and 2–4 (P2). (Da and Db–Ea and Eb) Analysis by IF to detect Cux1 (L2–4), Ctip2 (L5), and Tbr1 (L6) showed that Ctip2$^+$ L5 appeared thicker in *Tbr2* cKO cortex. Quantitatively, Cux1$^+$ cells were overall reduced (Dd; $p = 0.012$) and restricted to more-superficial bins (Dc) in *Tbr2* cKO cortex. In contrast, Ctip2$^+$ cells were greatly increased (Df; $p = 3.2 \times 10^{-8}$) and distributed within an expanded L5 (De) of *Tbr2* cKO mutants. Tbr1$^+$ neurons were moderately reduced (Ed; $p = 7.7 \times 10^{-4}$) and shifted. (*$p \leq 0.042$ in bin analyses). n = 3 WT and 3 cKO pups. The scale bar represents 100 μm (all images). All error bars represent SEM.

Also see Figure S5.

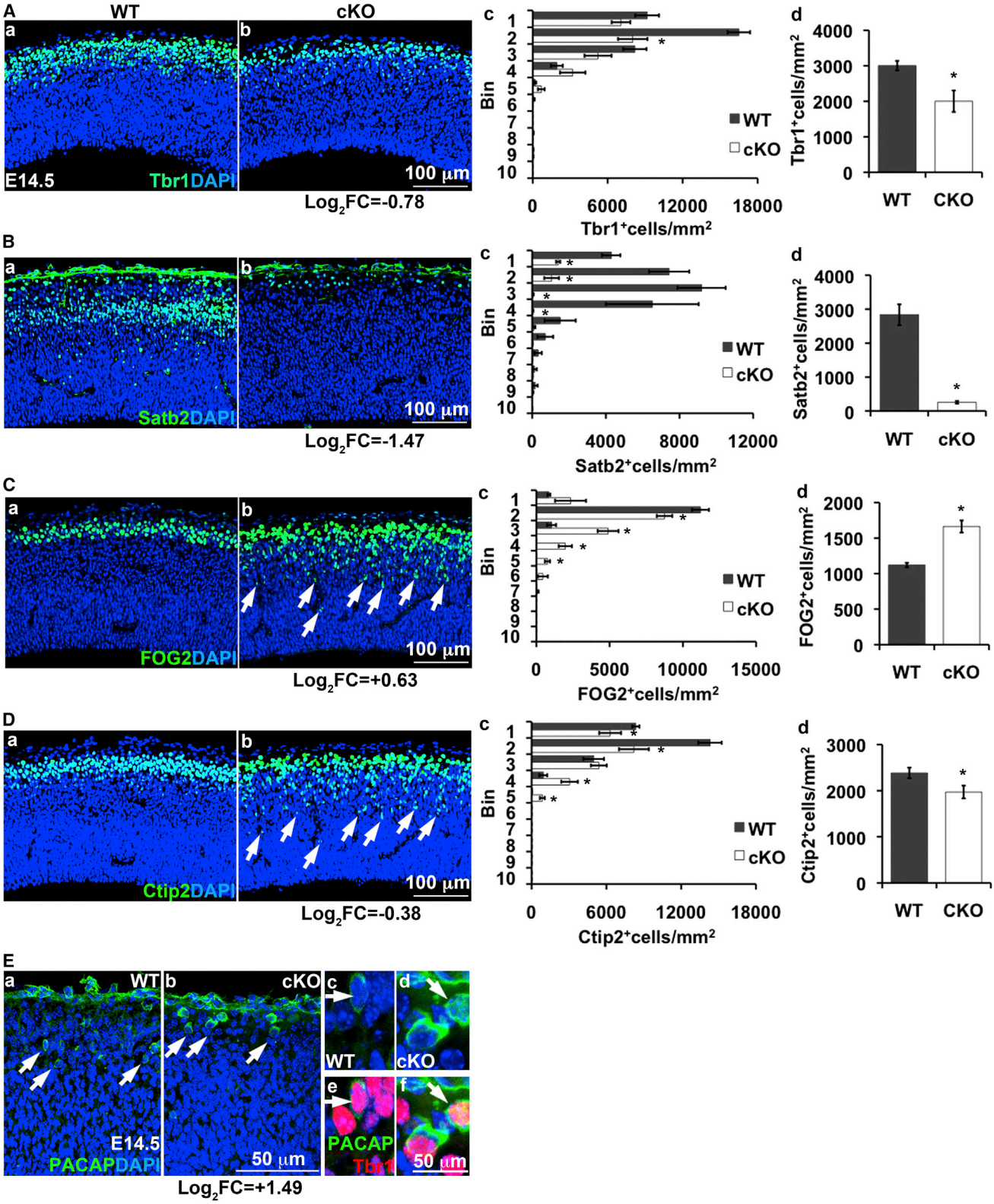

Figure 5. Zonal Expression Patterns of TFs that Regulate Projection Neuron Differentiation Are Altered in E14.5 *Tbr2* cKO Cortex

(Aa, Ab–Da, and Db) Expression of (A) Tbr1, (B) Satb2, (C) FOG2, and (D) Ctip2 in E14.5 control (Aa, Ba, Ca, and Da) and *Tbr2* cKO (Ab, Bb, Cb, and Db) cortex. (Ac, Bc, Cc, and Dc) Bin analysis of cells expressing each marker in WT and *Tbr2* cKO cortex, in bins spanning VZ to MZ (*p $\leq$ 0.049), is shown. Note ectopic

(legend continued on next page)

accumulation of immature neurons (Figure S6B). These results suggested that differentiation of preplate neurons was impaired in E12.5 *Tbr2* cKO mutants and early neurogenesis was increased (Figure 4A) in compensation.

In E16.5 *Tbr2* mutants, the numbers of Tbr1$^+$, Ctip2$^+$, and PACAP$^+$ LL neurons were strikingly increased over WT and CP thickness was increased (Figures S6C–S6E). PACAP$^+$ neurons also expressed Ctip2 (Figures S6E and S6F), supporting their identity as a subset of L5 neurons (Lodato et al., 2014). In contrast to increased LL thickness, UL thickness was decreased in E16.5 *Tbr2* cKO cortex compared to WT (Figures S6C and S6D) and ULs remained thin on P2 (Figures 4D and 4E).

Together with BrdU birth dating (Figures 4A–4C), these data indicated that early, middle, and late phases of cortical differentiation were severely abnormal in *Tbr2* cKO cortex. The delayed differentiation of early-born neurons (Figures S6A and S6B) may account for the shift from L6 to L5 fates (Figures 4D and 4E) and for the compensatory burst of early neurogenesis (Figure 4A) in *Tbr2* cKO mutants. In turn, excessive early neurogenesis may have depleted progenitors, leading to decreased neurogenesis by E14.5–E16.5 (Figures 4B and 4C) and consequent thinning of ULs (Figures 4D and 4E).

Basal Progenitors Are Dysregulated and Increased in Tbr2 cKO Cortex

The defects of neuronal differentiation in *Tbr2* cKO neocortex might be attributable to defective genesis and/or differentiation of IPs. To identify IPs and distinguish them from RGPs, we studied abventricular (basal) mitoses (AVMs) and ventricular (apical) mitoses (VMs) by phospho-histone H3 (pH3) IF (Kowalczyk et al., 2009).

In E12.5 *Tbr2* cKO mutants, the number of AVMs was unchanged from controls, but VMs were increased to 1.7-fold ($p = 4.4 \times 10^{-9}$) and S phase cells (acute BrdU$^+$) to 1.2-fold ($p = 0.0245$) of control values (Figures 6A–6E). By E14.5, VMs normalized but AVMs increased to significantly exceed control numbers (1.4-fold; $p = 4.7 \times 10^{-5}$; Figures 6F and 6G). Moreover, AVMs in *Tbr2* cKO cortex were not confined to the VZ/SVZ as in controls but were also found ectopically in the IZ and CP (Figures 6G and 6J). Furthermore, acute BrdU$^+$ (S phase) cells were also observed in the *Tbr2* cKO IZ and CP, and BrdU$^+$ cells in the VZ were disorganized (Figures 6G and 6H). Nevertheless, the total numbers of BrdU$^+$ cells were similar in E14.5 mutants and controls. These results indicated that basal IPs were not diminished but were actually increased in *Tbr2* cKO mutants, contradicting previous reports (Arnold et al., 2008; Sessa et al., 2008).

We next studied expression of Pax6 and Insm1, transcription factors upstream of *Tbr2* that promote genesis of Tbr2$^+$ IPs (Quinn et al., 2007; Farkas et al., 2008; Sansom et al., 2009). Strikingly, Pax6$^+$ and Insm1$^+$ cells were not only increased 1.4-fold ($p = 0.0011$) and 2.6-fold ($p = 4.3 \times 10^{-10}$), respectively, but were also located ectopically in the IZ and CP of *Tbr2* mutants (Figures 7A and 7B). Moreover, pH3$^+$ AVMs were more likely to express Pax6 (3.6-fold; $p = 0.024$) and Insm1 (24-fold; $p = 3 \times 10^{-5}$) in mutant than in control cortex (Figures 7C and 7D), suggesting that Tbr2-deficient IPs failed to downregulate these transcription factors (Englund et al., 2005; Farkas et al., 2008).

We next studied expression of NeuroD, a transcription factor expressed in basal IPs and newly generated neurons (Hevner et al., 2006). In E14.5 *Tbr2* cKO cortex, NeuroD was expressed by increased numbers of cells (1.2-fold; $p = 0.033$), including many in the IZ, SP, and CP, demonstrating ectopic expression of NeuroD in neuronal maturation zones (Figures 7E and S7A–S7D). The fraction of AVMs that expressed NeuroD was also increased in *Tbr2* cKO cortex relative to controls (1.7-fold; $p = 0.0105$; Figure 7E), consistent with protracted IP differentiation despite active NeuroD expression. Many NeuroD$^+$ cells aberrantly co-expressed Pax6 in *Tbr2* mutant cortex (25-fold more than in WT; Figures S7D and S7E). Thus, the differentiation of IPs and new neurons was disorganized and prolonged in *Tbr2* cKO cortex.

Together, these findings indicate that Tbr2 is not necessary for IP genesis but is required to promote the transition from IPs to postmitotic neurons (Figure 7F). In the absence of Tbr2, IP genesis continues, AVMs accumulate, and differentiation of IPs to neurons is profoundly abnormal.

DISCUSSION

In the present study, we found that IP cohorts make complex contributions to cortical layers, including an unexpected contribution from early IPs to upper cortical layers. We also showed that Tbr2 regulates laminar organization of the cortex by facilitating the transition from IP to neuron and promoting the timely acquisition of laminar identity.

The finding that some early IPs produce UL neurons (Figure 1A) suggested two possible interpretations. First, if laminar fate is specified in RGPs and some early RGPs have restricted UL fates (Franco et al., 2012), then early IPs inherit UL fates from parent RGPs. Alternatively, if IPs are initially multipotent with regard to laminar identities, then daughter neuron fates may be determined by the timing of final mitosis and limited by progressive fate restriction (Desai and McConnell, 2000). The latter possibility is favored by previous evidence that IPs can divide asymmetrically (with respect to laminar fate) to produce multiple layers (Wu et al., 2005). To resolve this issue, clonal analysis of IP lineages will be necessary.

Our findings challenge the previous conclusion that Tbr2 is required primarily for IP genesis (Sessa et al., 2008). Specifically,

expression of FOG2 in the IZ (arrows, Cb). (Ad, Bd, Cd, and Dd) Cell counts showed decreased Tbr1$^+$ ($p = 0.012$), Satb2$^+$ ($p = 5.8 \times 10^{-6}$), and Ctip2$^+$ ($p = 0.044$) cells in *Tbr2* cKO cortex, whereas FOG2$^+$ cells were increased ($p = 0.003$). Despite overall reduction, Ctip2$^+$ cells were located not only in the very thin CP but also ectopically in the IZ (D, arrows).

(E) PACAP$^+$ cells were larger and expressed higher levels of PACAP in *Tbr2* cKO (b) than in control cortex (a) and co-expressed Tbr1 (in E14.5 neocortex, a marker of all projection neurons) in both genotypes (c–f). Numbers under the (b) column indicate changes (log_2FC) in the expression of mRNA for each marker (all $p < 0.05$) in *Tbr2* cKO cortex. Positive numbers indicate increased and negative numbers decreased expression. $n \geq 3$ WT and 3 cKO embryos. Error bars represent SEM. Also see Figure S6.

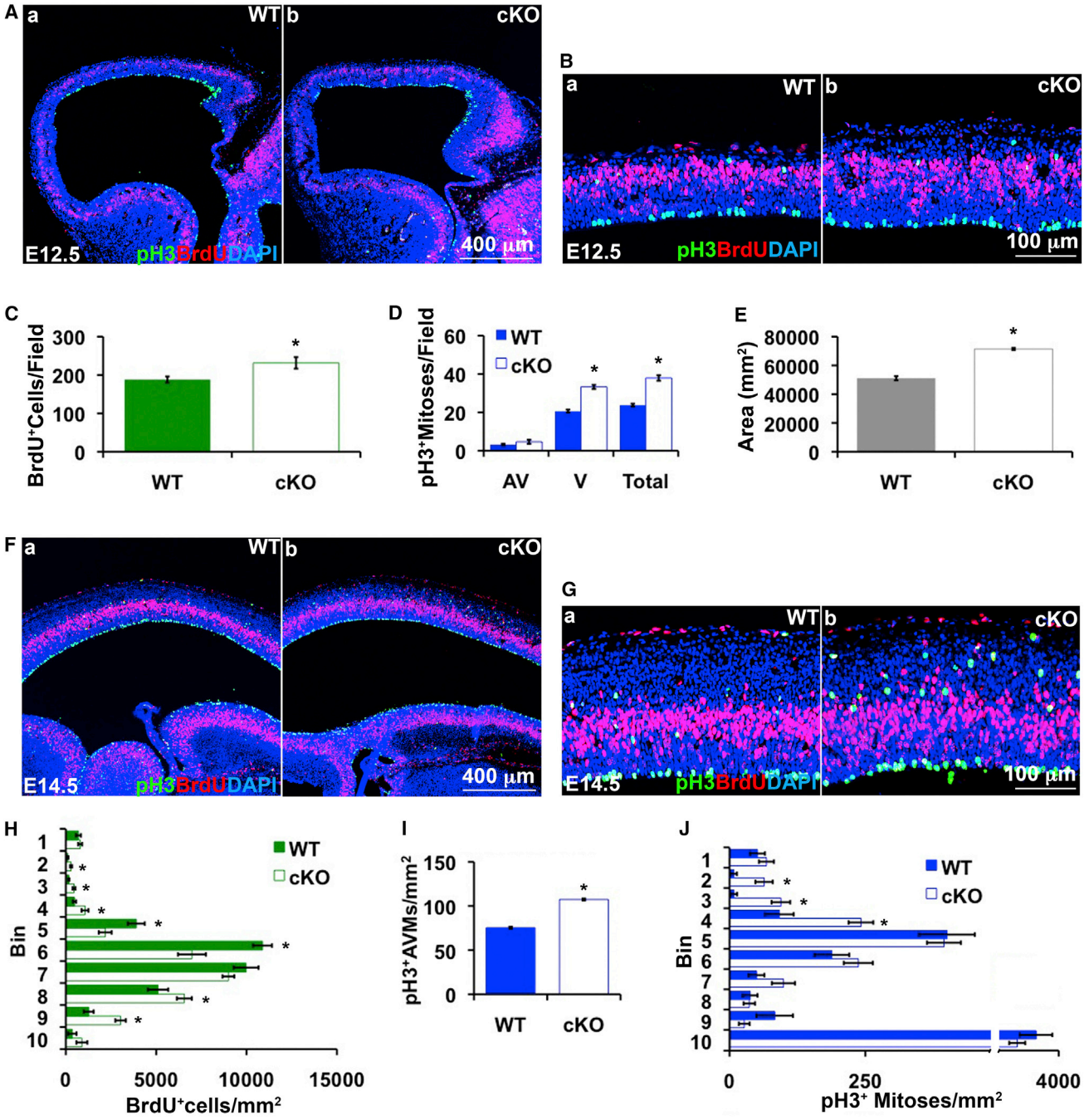

Figure 6. *Tbr2* cKO Cortex Has Increased Numbers of Basal/Abventricular Mitoses on E14.5

(A and B) E12.5 WT (a) and *Tbr2* cKO (b) cortex labeled with acute BrdU (red) and pH3 (green). Ba and Bb show higher magnifications of Aa and Ba, respectively.

(C and D) The number of $BrdU^+$ cells was increased in E12.5 *Tbr2* cKO cortex (C; $p = 0.024$), as was the total number of $pH3^+$ mitoses (D), due to an increase of VMs ($p < 1.2 \times 10^{-8}$) only. (VMs can be RGP or IP mitoses.)

(E) Cortical thickness (measured as area over a defined length of ventricular surface) was increased in the E12.5 *Tbr2* cKO cortex ($p = 8.4 \times 10^{-7}$), due mainly to preplate expansion.

(F and G) E14.5 WT (a) and *Tbr2* cKO (b) cortex labeled with acute BrdU (red) and pH3 (green). Ga and Gb show higher magnifications of Fa and Fb, respectively.

(H) The distribution of $BrdU^+$ cells was altered in E14.5 *Tbr2* cKO cortex, with increased numbers in abventricular (bins 2–4) and adventricular (bins 8–9) zones (*$p < 0.048$).

(I) The number of AVMs was overall increased in *Tbr2* cKO cortex ($p = 4.6 \times 10^{-5}$).

(J) $pH3^+$ AVMs were also shifted superficially, with increased numbers in bins 2–4 (IZ and CP; *$p \leq 0.005$); $n \geq 3$ WT and 3 cKO embryos. Error bars represent SEM.

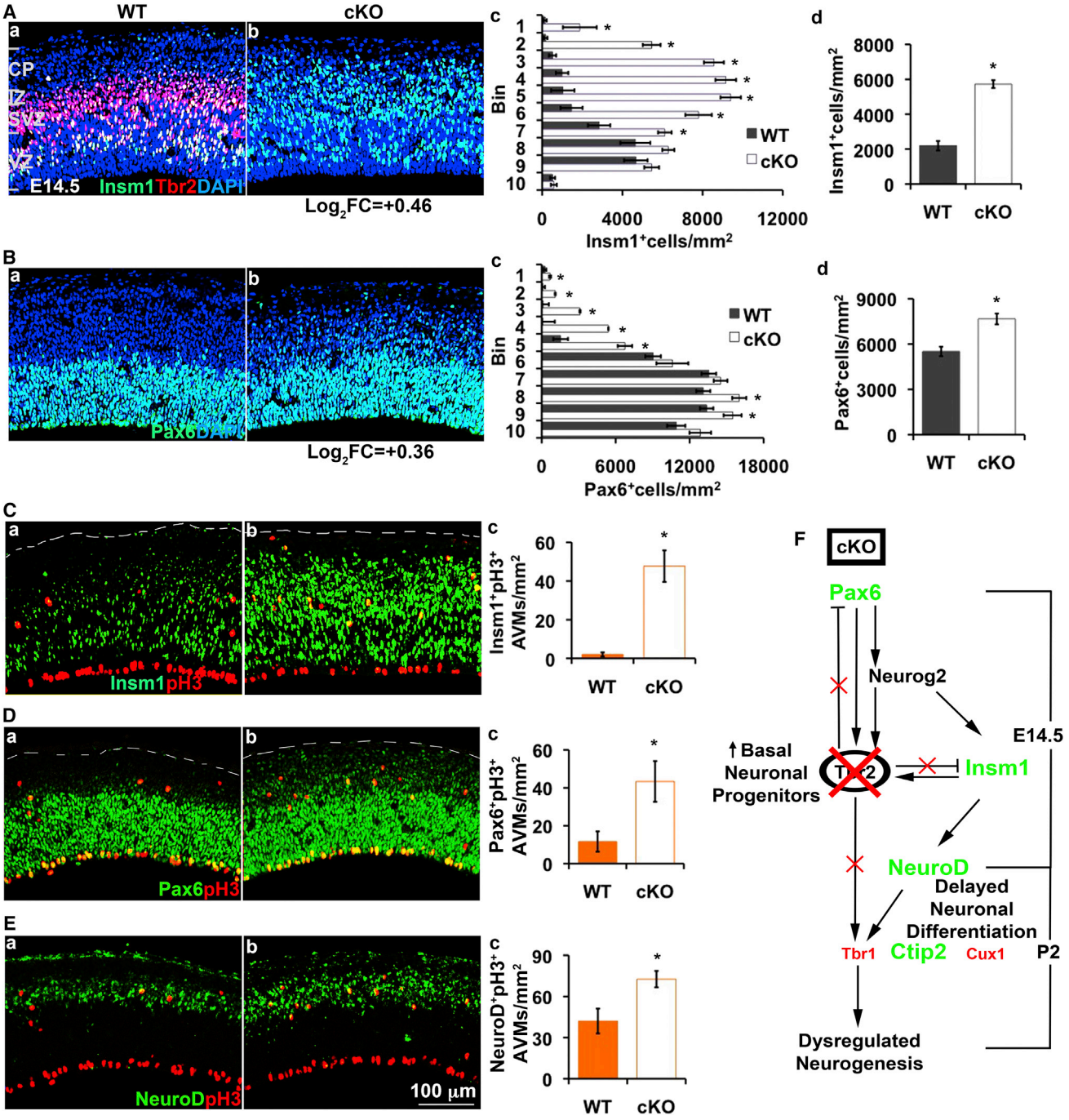

Figure 7. Tbr2-Deficient Basal IPs Express Insm1 and Pax6 Ectopically and NeuroD at Increased Levels

(A) Two-color IF to detect Tbr2 (red) and Insm1 (green) in E14.5 control (Aa) and *Tbr2* cKO (Ab) cortex showed increased numbers of Insm1$^+$ cells in Tbr2 cKO cortex (Ad; $p = 4.3 \times 10^{-10}$), especially in superficial bins (Ac) representing IZ and CP (*$p \leq 0.041$).

(B) Pax6 expression in E14.5 WT (Ba) and *Tbr2* cKO (Bb) cortex. Pax6$^+$ cells were found ectopically in the IZ and CP (Bc) and were overall increased (Bd; $p = 0.001$). Numbers under column (b) indicate changes in mRNA expression (log_2FC) between *Tbr2* cKO and control cortex from microarray analysis.

(C–E) Insm1$^+$, Pax6$^+$, and NeuroD$^+$ AVMs were increased in E14.5 *Tbr2* cKO cortex (b) relative to control (a), as confirmed by cell counting (c; Insm1$^+$ AVMs, $p = 3.0 \times 10^{-5}$; Pax6$^+$ AVMs, $p = 0.024$; NeuroD$^+$ AVMs, $p = 0.01$). $n \geq 3$ WT and 3 cKO embryos.

(F) Diagram illustrating the dysregulated TF network in E14.5 *Tbr2* cKO cortex and altered laminar fates in P2 *Tbr2* cKO cortex. Green-labeled TFs show increased, whereas red-labeled TFs show decreased, expression in *Tbr2* cKO. The scale bar represents 100 μm (all images). Error bars represent SEM.

Also see Figure S7.

we found that basal mitoses were not reduced but were actually increased in E14.5 *Tbr2* cKO neocortex (Figures 6F, 6G, and 6I). In contrast, previous studies reported that basal mitoses were significantly depleted in *Tbr2* cKO neocortex (Arnold et al., 2008; Sessa et al., 2008). We attribute these discrepancies to different Cre drivers and floxed *Tbr2* alleles. The previous study implicating Tbr2 in IP genesis (Sessa et al., 2008) used *Foxg1*^{Cre}, a knockin allele that itself causes IP depletion (Siegenthaler et al., 2008). Another previous study (Arnold et al., 2008) used *Sox1*^{Cre}, likewise a knockin allele (Takashima et al., 2007) that causes defects of brain development and function (Malas et al., 2003). In contrast, *Nes11*^{Cre}, used in the present study, is a transgene that does not directly interfere with gene expression or with brain development and function (Tronche et al., 1999).

The aberrant and protracted differentiation of neurons in embryonic *Tbr2* cKO cortex can be traced to gene dysregulation in IPs. The ectopic expression of Pax6 and Insm1 in *Tbr2* cKO IZ and CP (Figure 7) suggests that Tbr2 is required to downregulate these transcription factors, possibly by direct transcriptional repression in IPs. Indeed, Tbr2 binding sites are found near the *Pax6* and *Insm1* promoters (Teo et al., 2011). The persistent expression of Pax6 and Insm1 may interfere with neuronal differentiation in cortex, as demonstrated for ectopic Pax6 in the spinal cord (Bel-Vialar et al., 2007). Thus, Tbr2 appears to facilitate neuronal differentiation in part by repressing molecules that are normally expressed only in progenitor cells.

Conversely, Tbr2 may direct neuronal maturation by activating transcription of molecules expressed in differentiating neurons, such as Tbr1 and Satb2. Consistent with this possibility, both Satb2 and Tbr1 are initially detected in basal IPs, albeit at low levels (Britanova et al., 2005; Nelson et al., 2013). On the other hand, some important neuronal differentiation factors (such as NeuroD) are clearly not dependent on Tbr2. Also, despite abnormal gene expression in the *Tbr2* cKO cortex, most projection neurons ultimately differentiated successfully. Indeed, the *Tbr2* cKO cortex underwent a marked change between E14.5, when the CP was thin with a paucity of Tbr1$^+$ neurons (Figure 5A), and E16.5, when the CP was thick with abundant Tbr1$^+$ and Ctip2$^+$ neurons (Figures S6C and S6D). The number of Satb2$^+$ neurons likewise recovered substantially after E14.5 (Figure S6I). In the absence of Tbr2, upregulation of other molecules, such as NeuroD (Figures S7A–S7D), may compensate to ensure neuronal differentiation.

Tbr2 appears to regulate laminar fate by multiple mechanisms. Inactivation of *Tbr2* in IP cohorts (E12.5 and E14.5) led to reduced genesis of rapidly generated neuron subtypes (deeper in cortex) and relatively increased genesis of later-generated subtypes (more superficial; Figure 3). Because Tbr2-deficient cohorts were sparse, these results indicated that Tbr2 is required cell autonomously for rapid IP differentiation and neurogenesis. Extrapolating from these findings, *Tbr2* cKO (throughout cortex) may have delayed the differentiation of all IP cohorts, causing an overall shift away from early-born neuron subtypes toward increased genesis of later-born subtypes. Indeed, Tbr1$^+$ neurons and L6 thickness were decreased in *Tbr2* cKO mice (Figure 4E). However, Tbr2 may also regulate the balance of L6 and L5 fates directly: E12.5-born (BrdU$^+$) cells were more likely to differentiate as Ctip2$^+$ neurons in *Tbr2* cKO cortex (Figure S5Bc), and L5 markers PACAP and Ctip2 were markedly increased by E16.5 in *Tbr2* cKO cortex (Figures S6D–S6F). Thus, Tbr2 appears to directly regulate both the rate of IP differentiation and the balance of L6 and L5 fates during early neurogenesis.

Despite the delayed differentiation of IPs, neurogenesis was initially accelerated in E12.5 *Tbr2* cKO cortex but decreased subsequently on E14.5 and E16.5 (Figures 4A–4C). The acceleration of early neurogenesis may represent a non-autonomous effect of altered IP differentiation. Such effects are anticipated because IPs interact with RGPs, for example, by Delta-Notch signaling (Nelson et al., 2013). We speculate that deficient Delta-Notch signaling in early *Tbr2* cKO cortex caused RGPs to respond by increasing direct neurogenesis (Figure 4A) and overproducing preplate neurons (Figures S6A and S6B). In turn, the RGP pool may have been depleted prematurely in *Tbr2* cKO mutants, thus accounting for reduced genesis of late-born UL neurons and decreased UL thickness (Figures 4B–4D). In sum, laminar defects in *Tbr2* cKO cortex reflect a complex system of differentiation and feedback.

Interestingly, the reduction of late neurogenesis and UL thickness occurred despite ample production of basal progenitors in *Tbr2* cKO cortex (Figure 6I). Previous studies have shown that IP genesis is driven by low Notch signaling in RGPs (Nelson et al., 2013) and by neurogenic transcription factors, including Pax6, Insm1, and Neurog2 (Sun and Hevner, 2014). Those "upstream" mechanisms of IP specification occur in RGPs prior to the expression of Tbr2, so our finding that IP genesis was spared in *Tbr2* cKO cortex is logical. Rather, Tbr2 deficiency perturbed gene expression in new IPs and impaired their ability to differentiate as cortical projection neurons with well-defined laminar subtype identities. Our findings indicate that Tbr2 plays an important transitional role in neurogenesis by both suppressing RGP identity and promoting specific features of cortical layers. Ultimately, neuronal differentiation and layer formation were delayed in *Tbr2* cKO mice but proceeded to completion due to compensatory mechanisms.

Remarkably, major motor skills were not impaired in *Tbr2* cKO mice (Figures S5C and S5E), although previous studies detected hyperactivity and weakness (Arnold et al., 2008). The small olfactory bulb and rudimentary dentate gyrus in *Tbr2* mutants (Hodge et al., 2013) presumably impair olfaction and memory, but those functions have not been tested. Interestingly, *Nlgn3* mutant mice also show improved performance on repetitive motor tasks (Rothwell et al., 2014).

In sum, we have shown that IPs can persist in the cortex for prolonged periods and that early IP cohorts contribute to multiple cortical layers. The pace of laminar neurogenesis and the identities of projection neurons are regulated by Tbr2, although the genesis of IPs is not. In future studies, it will be interesting to conduct clonal analysis of IP progeny and determine whether individual IPs contribute to multiple layers as well as the size and distribution of IP-derived clones.

EXPERIMENTAL PROCEDURES

Animals and Tissue Collection

C57BL/6 mice used in this study were kept in a 12 hr light/dark cycle, with food and water ad libitum, in Seattle Children's Research Institute's vivarium. All

animal experimental procedures were performed with Institutional Animal Care and Use Committee approval. The following previously described mouse transgenic alleles were used: *Ai14* reporter (Madisen et al., 2010); *Eomes*^{CreER} (*Tbr2*^{CreER}; Pimeisl et al., 2013); *Nestin*-Cre (*Nes11*^{Cre}; Tronche et al., 1999; stock 003771; The Jackson Laboratory); and *Tbr2-Flox* (*Tbr2*^{FL}; Intlekofer et al., 2008). Also see Supplemental Experimental Procedures.

Tam and BrdU Administration

Pregnant dams were administered Tam (Sigma; T5648; 5 mg/kg), progesterone (Sigma; P3972; 2.5 mg/kg), and BrdU (Sigma; B5002; 50 mg/kg) by intraperitoneal injection at the indicated embryonic ages. Acute BrdU treatment was done 30 min before brain collection.

IF

The IF procedure was previously described (Englund et al., 2005). Also see Supplemental Experimental Procedures.

Image Acquisition, Cell Counting, and Statistics

Single-plane optical sections and stacks were acquired with Zeiss LSM-710 confocal microscope. Cell counts were reported either as absolute number or density per area (mm^2) or as distribution per bin/cortical zone. Also see Supplemental Experimental Procedures. Data were reported as mean ± SEM from at least three sections from an animal and two to four animals per condition/data point. Statistical analysis used two-tailed, unpaired Student's t test, and the confidence threshold chosen is $p < 0.05$.

Rotarod

Male mice between 6 weeks and 6 months of age were tested on the Rotamex-5 (Columbus Instruments) for rotarod performance to assess their motor skills as described (Hsu et al., 2014). Also see Supplemental Experimental Procedures.

Balance Beam

Tbr2 cKO and littermate control male mice, 3–4 months of age, were used in the balance beam test, as described (Hsu et al., 2014). Also see Supplemental Experimental Procedures.

Microarrays

Data from our previous microarray experiment (http://www.ncbi.nlm.nih.gov/geo; GEO: GSE43387; Elsen et al., 2013) were analyzed in the present study. Also see Supplemental Experimental Procedures.

SUPPLEMENTAL INFORMATION

Supplemental Information includes Supplemental Experimental Procedures and seven figures and can be found with this article online at http://dx.doi.org/10.1016/j.celrep.2016.05.072.

AUTHOR CONTRIBUTIONS

A.B.M. and R.F.H. designed the study and wrote the manuscript. A.B.M., R.A.M.D., K.A.R.-L., G.E.E., and F.B. performed experiments. S.J.A. provided research materials and manuscript editing/commenting. A.B.M. and R.F.H. analyzed data.

ACKNOWLEDGMENTS

We thank E. Young and L. Honican for assistance with experiments and analysis. We thank Dr. C. Birchmeier (Max-Delbrück-Center for Molecular Medicine) for Insm1 antibody, Dr. J. Kohtz (Northwestern University) for Dlx antibody, and Dr. J. Hannibal for PACAP antibody (University of Copenhagen). We thank Dr. T. Bammler, Dr. F. Farin, and Dr. D. Beyer (University of Washington Center for Ecogenetics and Environmental Health) for assistance with microarray experiments and the UW Center on Human Development and Disability for partial support of microarray experiments (supported by grant U54 HD083091 from the National Institute of Child Health and Human Development to the University of Washington's Center on Human Development and Disability). This study was supported by NIH grants R01 NS085081 and R01 NS092339 to R.F.H., German Research Foundation (DFG) Emmy Noether Programme (AR732/1-1) to S.J.A., and Lejeune Foundation and ProRett Italia to F.B.

Received: November 25, 2015
Revised: March 28, 2016
Accepted: May 16, 2016
Published: June 16, 2016

REFERENCES

Arnold, S.J., Huang, G.J., Cheung, A.F., Era, T., Nishikawa, S., Bikoff, E.K., Molnár, Z., Robertson, E.J., and Groszer, M. (2008). The T-box transcription factor Eomes/Tbr2 regulates neurogenesis in the cortical subventricular zone. Genes Dev. *22*, 2479–2484.

Bedogni, F., Hodge, R.D., Elsen, G.E., Nelson, B.R., Daza, R.A., Beyer, R.P., Bammler, T.K., Rubenstein, J.L., and Hevner, R.F. (2010). Tbr1 regulates regional and laminar identity of postmitotic neurons in developing neocortex. Proc. Natl. Acad. Sci. USA *107*, 13129–13134.

Bel-Vialar, S., Medevielle, F., and Pituello, F. (2007). The on/off of Pax6 controls the tempo of neuronal differentiation in the developing spinal cord. Dev. Biol. *305*, 659–673.

Britanova, O., Akopov, S., Lukyanov, S., Gruss, P., and Tarabykin, V. (2005). Novel transcription factor Satb2 interacts with matrix attachment region DNA elements in a tissue-specific manner and demonstrates cell-type-dependent expression in the developing mouse CNS. Eur. J. Neurosci. *21*, 658–668.

Bystron, I., Blakemore, C., and Rakic, P. (2008). Development of the human cerebral cortex: Boulder Committee revisited. Nat. Rev. Neurosci. *9*, 110–122.

Desai, A.R., and McConnell, S.K. (2000). Progressive restriction in fate potential by neural progenitors during cerebral cortical development. Development *127*, 2863–2872.

Elsen, G.E., Hodge, R.D., Bedogni, F., Daza, R.A., Nelson, B.R., Shiba, N., Reiner, S.L., and Hevner, R.F. (2013). The protomap is propagated to cortical plate neurons through an Eomes-dependent intermediate map. Proc. Natl. Acad. Sci. USA *110*, 4081–4086.

Englund, C., Fink, A., Lau, C., Pham, D., Daza, R.A., Bulfone, A., Kowalczyk, T., and Hevner, R.F. (2005). Pax6, Tbr2, and Tbr1 are expressed sequentially by radial glia, intermediate progenitor cells, and postmitotic neurons in developing neocortex. J. Neurosci. *25*, 247–251.

Farkas, L.M., Haffner, C., Giger, T., Khaitovich, P., Nowick, K., Birchmeier, C., Pääbo, S., and Huttner, W.B. (2008). Insulinoma-associated 1 has a panneurogenic role and promotes the generation and expansion of basal progenitors in the developing mouse neocortex. Neuron *60*, 40–55.

Florio, M., and Huttner, W.B. (2014). Neural progenitors, neurogenesis and the evolution of the neocortex. Development *141*, 2182–2194.

Franco, S.J., Gil-Sanz, C., Martinez-Garay, I., Espinosa, A., Harkins-Perry, S.R., Ramos, C., and Müller, U. (2012). Fate-restricted neural progenitors in the mammalian cerebral cortex. Science *337*, 746–749.

Gal, J.S., Morozov, Y.M., Ayoub, A.E., Chatterjee, M., Rakic, P., and Haydar, T.F. (2006). Molecular and morphological heterogeneity of neural precursors in the mouse neocortical proliferative zones. J. Neurosci. *26*, 1045–1056.

Hevner, R.F., Daza, R.A., Rubenstein, J.L., Stunnenberg, H., Olavarria, J.F., and Englund, C. (2003). Beyond laminar fate: toward a molecular classification of cortical projection/pyramidal neurons. Dev. Neurosci. *25*, 139–151.

Hevner, R.F., Hodge, R.D., Daza, R.A., and Englund, C. (2006). Transcription factors in glutamatergic neurogenesis: conserved programs in neocortex, cerebellum, and adult hippocampus. Neurosci. Res. *55*, 223–233.

Hodge, R.D., Garcia, A.J., 3rd, Elsen, G.E., Nelson, B.R., Mussar, K.E., Reiner, S.L., Ramirez, J.M., and Hevner, R.F. (2013). Tbr2 expression in Cajal-Retzius cells and intermediate neuronal progenitors is required for morphogenesis of the dentate gyrus. J. Neurosci. *33*, 4165–4180.

Hsu, Y.W., Wang, S.D., Wang, S., Morton, G., Zariwala, H.A., de la Iglesia, H.O., and Turner, E.E. (2014). Role of the dorsal medial habenula in the regulation of voluntary activity, motor function, hedonic state, and primary reinforcement. J. Neurosci. *34*, 11366–11384.

Intlekofer, A.M., Banerjee, A., Takemoto, N., Gordon, S.M., Dejong, C.S., Shin, H., Hunter, C.A., Wherry, E.J., Lindsten, T., and Reiner, S.L. (2008). Anomalous type 17 response to viral infection by CD8+ T cells lacking T-bet and eomesodermin. Science *321*, 408–411.

Kawaguchi, A., Ikawa, T., Kasukawa, T., Ueda, H.R., Kurimoto, K., Saitou, M., and Matsuzaki, F. (2008). Single-cell gene profiling defines differential progenitor subclasses in mammalian neurogenesis. Development *135*, 3113–3124.

Kowalczyk, T., Pontious, A., Englund, C., Daza, R.A., Bedogni, F., Hodge, R., Attardo, A., Bell, C., Huttner, W.B., and Hevner, R.F. (2009). Intermediate neuronal progenitors (basal progenitors) produce pyramidal-projection neurons for all layers of cerebral cortex. Cereb. Cortex *19*, 2439–2450.

Lodato, S., Molyneaux, B.J., Zuccaro, E., Goff, L.A., Chen, H.H., Yuan, W., Meleski, A., Takahashi, E., Mahony, S., Rinn, J.L., et al. (2014). Gene co-regulation by Fezf2 selects neurotransmitter identity and connectivity of corticospinal neurons. Nat. Neurosci. *17*, 1046–1054.

Madisen, L., Zwingman, T.A., Sunkin, S.M., Oh, S.W., Zariwala, H.A., Gu, H., Ng, L.L., Palmiter, R.D., Hawrylycz, M.J., Jones, A.R., et al. (2010). A robust and high-throughput Cre reporting and characterization system for the whole mouse brain. Nat. Neurosci. *13*, 133–140.

Malas, S., Postlethwaite, M., Ekonomou, A., Whalley, B., Nishiguchi, S., Wood, H., Meldrum, B., Constanti, A., and Episkopou, V. (2003). Sox1-deficient mice suffer from epilepsy associated with abnormal ventral forebrain development and olfactory cortex hyperexcitability. Neuroscience *119*, 421–432.

Molyneaux, B.J., Arlotta, P., Menezes, J.R., and Macklis, J.D. (2007). Neuronal subtype specification in the cerebral cortex. Nat. Rev. Neurosci. *8*, 427–437.

Nelson, B.R., Hodge, R.D., Bedogni, F., and Hevner, R.F. (2013). Dynamic interactions between intermediate neurogenic progenitors and radial glia in embryonic mouse neocortex: potential role in Dll1-Notch signaling. J. Neurosci. *33*, 9122–9139.

Pimeisl, I.M., Tanriver, Y., Daza, R.A., Vauti, F., Hevner, R.F., Arnold, H.H., and Arnold, S.J. (2013). Generation and characterization of a tamoxifen-inducible Eomes(CreER) mouse line. Genesis *51*, 725–733.

Quinn, J.C., Molinek, M., Martynoga, B.S., Zaki, P.A., Faedo, A., Bulfone, A., Hevner, R.F., West, J.D., and Price, D.J. (2007). Pax6 controls cerebral cortical cell number by regulating exit from the cell cycle and specifies cortical cell identity by a cell autonomous mechanism. Dev. Biol. *302*, 50–65.

Rothwell, P.E., Fuccillo, M.V., Maxeiner, S., Hayton, S.J., Gokce, O., Lim, B.K., Fowler, S.C., Malenka, R.C., and Südhof, T.C. (2014). Autism-associated neuroligin-3 mutations commonly impair striatal circuits to boost repetitive behaviors. Cell *158*, 198–212.

Sansom, S.N., Griffiths, D.S., Faedo, A., Kleinjan, D.J., Ruan, Y., Smith, J., van Heyningen, V., Rubenstein, J.L., and Livesey, F.J. (2009). The level of the transcription factor Pax6 is essential for controlling the balance between neural stem cell self-renewal and neurogenesis. PLoS Genet. *5*, e1000511.

Sessa, A., Mao, C.A., Hadjantonakis, A.K., Klein, W.H., and Broccoli, V. (2008). Tbr2 directs conversion of radial glia into basal precursors and guides neuronal amplification by indirect neurogenesis in the developing neocortex. Neuron *60*, 56–69.

Siegenthaler, J.A., Tremper-Wells, B.A., and Miller, M.W. (2008). Foxg1 haploinsufficiency reduces the population of cortical intermediate progenitor cells: effect of increased p21 expression. Cereb. Cortex *18*, 1865–1875.

Stancik, E.K., Navarro-Quiroga, I., Sellke, R., and Haydar, T.F. (2010). Heterogeneity in ventricular zone neural precursors contributes to neuronal fate diversity in the postnatal neocortex. J. Neurosci. *30*, 7028–7036.

Stoykova, A., Hatano, O., Gruss, P., and Götz, M. (2003). Increase in reelin-positive cells in the marginal zone of Pax6 mutant mouse cortex. Cereb. Cortex *13*, 560–571.

Sun, T., and Hevner, R.F. (2014). Growth and folding of the mammalian cerebral cortex: from molecules to malformations. Nat. Rev. Neurosci. *15*, 217–232.

Takashima, Y., Era, T., Nakao, K., Kondo, S., Kasuga, M., Smith, A.G., and Nishikawa, S. (2007). Neuroepithelial cells supply an initial transient wave of MSC differentiation. Cell *129*, 1377–1388.

Tarabykin, V., Stoykova, A., Usman, N., and Gruss, P. (2001). Cortical upper layer neurons derive from the subventricular zone as indicated by Svet1 gene expression. Development *128*, 1983–1993.

Teo, A.K., Arnold, S.J., Trotter, M.W., Brown, S., Ang, L.T., Chng, Z., Robertson, E.J., Dunn, N.R., and Vallier, L. (2011). Pluripotency factors regulate definitive endoderm specification through eomesodermin. Genes Dev. *25*, 238–250.

Tronche, F., Kellendonk, C., Kretz, O., Gass, P., Anlag, K., Orban, P.C., Bock, R., Klein, R., and Schütz, G. (1999). Disruption of the glucocorticoid receptor gene in the nervous system results in reduced anxiety. Nat. Genet. *23*, 99–103.

Tyler, W.A., Medalla, M., Guillamon-Vivancos, T., Luebke, J.I., and Haydar, T.F. (2015). Neural precursor lineages specify distinct neocortical pyramidal neuron types. J. Neurosci. *35*, 6142–6152.

Vasistha, N.A., García-Moreno, F., Arora, S., Cheung, A.F., Arnold, S.J., Robertson, E.J., and Molnár, Z. (2015). Cortical and clonal contribution of Tbr2 expressing progenitors in the developing mouse brain. Cereb. Cortex *25*, 3290–3302.

Wu, S.X., Goebbels, S., Nakamura, K., Nakamura, K., Kometani, K., Minato, N., Kaneko, T., Nave, K.A., and Tamamaki, N. (2005). Pyramidal neurons of upper cortical layers generated by NEX-positive progenitor cells in the subventricular zone. Proc. Natl. Acad. Sci. USA *102*, 17172–17177.

Zimmer, C., Tiveron, M.C., Bodmer, R., and Cremer, H. (2004). Dynamics of Cux2 expression suggests that an early pool of SVZ precursors is fated to become upper cortical layer neurons. Cereb. Cortex *14*, 1408–1420.